Active paradigms of seizure anticipation: Computer model evidence for necessity of stimulation

Piotr Suffczynski,[1] Stiliyan Kalitzin,[2] Fernando Lopes da Silva,[3] Jaime Parra,[4]
Demetrios Velis,[4] and Fabrice Wendling[5,6]

[1]*Department of Biomedical Physics, Faculty of Physics, University of Warsaw, 00-681 Warsaw, Poland*
[2]*Dutch Epilepsy Clinics Foundation (SEIN), Medical Physics Department, 2103 SW Heemstede, The Netherlands*
[3]*Swammerdam Institute of Life Sciences, Faculty of Biology, University of Amsterdam, 1098 SM, Amsterdam, The Netherlands and Instituto Superior Técnico, Universidade Técnica de Lisboa, 1049–001 Lisboa, Portugal*
[4]*Dutch Epilepsy Clinics Foundation (SEIN), Department of Clinical Neurophysiology, 2103 SW Heemstede, The Netherlands*
[5]*INSERM U642, Rennes, F-35000, France*
[6]*Universite de Rennes 1, LTSI, F-35000, France*

(Received 21 March 2008; revised manuscript received 24 June 2008; published 19 November 2008)

It has been shown that the analysis of electroencephalographic (EEG) signals submitted to an appropriate external stimulation (active paradigm) is efficient with respect to anticipating epileptic seizures [S. Kalitzin *et al.*, Clin. Neurophysiol. **116**, 718 (2005)]. To better understand how an active paradigm is able to detect properties of EEG signals by means of which proictal states can be identified, we performed a simulation study using a computational model of seizure generation of a hippocampal network. Applying the active stimulation methodology, we investigated (i) how changes in model parameters that lead to a transition from the normal ongoing EEG to an ictal pattern are reflected in the properties of the simulated EEG output signals and (ii) how the evolution of neuronal excitability towards seizures can be reconstructed from EEG data using an active paradigm, rather than passively, using only ongoing EEG signals. The simulations indicate that a stimulation paradigm combined with appropriate analytical tools, as proposed here, may yield information about the change in excitability that precedes the transition to a seizure. Such information is apparently not fully reflected in the ongoing EEG activity. These findings give strong support to the development and application of active paradigms with the aim of predicting the occurrence of a transition to an epileptic seizure.

DOI: 10.1103/PhysRevE.78.051917 PACS number(s): 87.85.eg, 87.19.xm

I. INTRODUCTION

Can epileptic seizures be predicted? A number of prediction algorithms have been proposed to date, but no method has been shown to perform good enough to be applied in clinical practice [1,2]. The majority of approaches are based on the concept that a *preictal* state—i.e., the state of the brain that precedes the occurrence of an epileptic seizure—has special properties and that the latter may be detected on ongoing electroencephalographic (EEG) signals. Accordingly, methods able to detect such a preictal state in the electroencephalogram of epileptic patients are being sought. Such approaches are based on two main assumptions. The first is that the seizures are preceded by specific changes in signal properties detectable in ongoing—i.e., spontaneous—EEG activity, and the second is that those changes represent a necessary and sufficient condition for a seizure to follow. It is important to note that the second assumption implies a deterministic relation, which, however, may not hold in general. The brain dynamics contains stochastic components that make this relationship complex. It has been suggested [3] that instead of searching for a method that may detect a specific preictal state in a deterministic way, one should preferably assume that it may be possible to estimate the probability of the occurrence of a change in the dynamical state of the brain that precedes a seizure. Thus it may be possible to calculate the probability that a subject will have a seizure some time in advance. In this context we assume the existence of a *proictal* state that is associated with a high risk of approaching a seizure. Novel seizure prediction schemes should take into account that states of high seizure probability do not necessarily lead to a seizure, but on the contrary, may evolve back to the interictal state [4]. It is also not obvious whether the first assumption, that the *passive* observation of spontaneous EEG activity is sufficient to reveal the susceptibility for seizures, holds in general. As an alternative, *active* paradigms based on stimulation of the brain and on analyzing the elicited responses have been proposed [5]. It has been shown that both in photosensitive [6] and in temporal lobe epilepsy (TLE) patients [3], the transition to a seizure can be reliably anticipated using EEG signal features derived from the response elicited by external stimulation, rather than only using information extracted from EEG spontaneous activity.

To obtain a deeper insight into the nature of the EEG changes leading to an ictal transition and into the reasons why a stimulation or "active" paradigm may be superior to a "passive" analysis, we investigated these processes using a computational approach. Therefore we constructed a realistic computational model of a hippocampal network. Accordingly we were able to investigate functional links between physiological parameters controlling excitability of the hippocampal network, on the one hand, and EEG quantities measured from passive observations or from the responses to active stimulations, on the other hand. Using the model, we demonstrated that changes during the transition to a seizure may be reconstructed more accurately using the active than the passive paradigm.

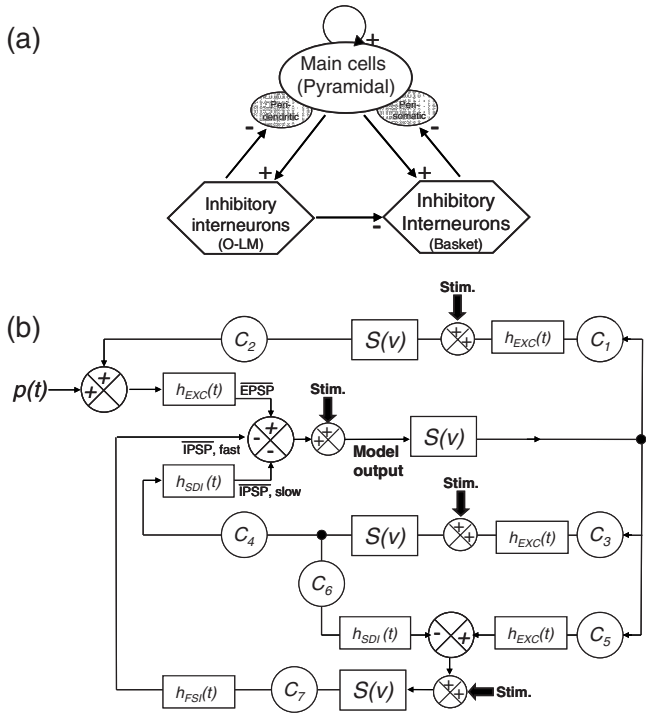

FIG. 1. Neuronal population model based on the cellular organization of the hippocampus (CA1 subfield). (a). Structure of model which represents a cluster of neurons composed of three subpopulations: main cells (i.e., pyramidal cells) and local interneurons (i.e., O-LM or basket cells). Pyramidal cells receive excitatory input from other pyramidal cells (collateral excitation) and inhibitory input from interneurons. (b). Block diagram representation of the model. $S(v)$ denote "wave-to-pulse" functions (asymmetric sigmoid curve), while $h_{EXC}(t)$, $h_{SDI}(t)$, and $h_{FSI}(t)$ denote "pulse-to-wave" functions (see text). The external stimulation was represented by an additive model between the output of "pulse-to-wave" functions and the potential difference induced by the extracellular bipolar stimulation electrode "Stim."

II. METHODS

A. Computational model

We used a computational model of the hippocampal network (CA1 subfield) developed by Wendling *et al.* [7,8]. We assumed that such a model would be an appropriate tool that could provide insight into the dynamics of real intracerebral EEG data that were recorded from the hippocampus of patients with TLE [3]. In this model a "lumped" approach was followed, according to which a macroscopic level of description—i.e., at the level of a neuronal population—is considered. For the hippocampus, this population consists of three subpopulations of neurons: the main (pyramidal) cells and the local inhibitory interneurons (O-LM and basket cells) projecting to either the dendritic or the perisomatic region of pyramidal cells, as illustrated in the schematic diagram of the model provided in Fig. 1(a). Input to interneurons is excitatory (glutamate receptor mediated). Feedback to pyramidal cells is either excitatory (glutamate receptor mediated) or inhibitory (GABA receptor mediated). Slow ($GABA_{A,slow}$) and fast ($GABA_{A,fast}$) kinetics are associated with inhibitory post-synaptic potentials (PSP) depending on the location of GABA receptors, in the dendritic or in the perisomatic region of pyramidal cells, respectively. A block diagram representation of the model is shown in Fig. 1(b). Basically, the model can be viewed as a nonlinear dynamical system driven by a Gaussian input noise $p(t)$ that globally represents the average density of afferent action potentials from neighboring or distant populations. Interactions between subpopulations of neurons are summarized in the model by connectivity constants $C1-C7$, which account for the average number of synaptic contacts. In each subpopulation, membrane potential is converted into an average pulse density of potentials fired by the neurons using a static nonlinear function $S(v)=2e_0/[1+e^{r(v_0-v)}]$ (asymmetric sigmoid curve), also referred to as the "wave-to-pulse" function. Conversely, the average pulse density of afferent action potentials is changed into an average inhibitory or excitatory postsynaptic membrane potential using a linear dynamic transfer function of impulse response $h_{EXC}(t)$, $h_{SDI}(t)$, and $h_{FSI}(t)$, the shape of which was shown to approximate that of actual postsynaptic potentials [9]. In these "pulse-to-wave" functions, EXC, SDI, and FSI denote the three main parameters of the model, which, respectively, correspond to the amplitude of average (i) excitatory PSPs (EXC), (ii) slow dendritic inhibitory PSPs (SDI), and (iii) fast somatic inhibitory PSPs (FSI). The model output corresponds to the summation of these average PSPs on pyramidal cells, which is known to be the principal contribution to local field potentials. From the mathematical viewpoint, each of the three impulse response h functions has the general form $h_G(t)=\frac{G}{\tau_G}te^{-t/\tau_G}$, where G denotes EXC, SDI, or FSI depending on the excitatory or inhibitory case and τ_G is a time constant. Each of the h functions is the impulse response solution of a second-order ordinary differential equation (ODE), which is equivalent to two first-order ODEs and thus the whole model reduces to a set of eight ODEs. The value and the meaning of each model parameter are given in Table I. Readers may refer to previous reports [8] for more detailed presentations. The model is also available online [10]. With respect to previous work, a novelty is that we reproduced, in the model, the effect of the external stimulation. We assumed that the extracellular bipolar stimulation electrode would produce a change of membrane potential proportional to the generated extracellular current in all three subpopulations represented in the model. In this way we neglected capacitive effects of the neurons' membrane for the sake of simplicity. Additionally we introduced another simplification—namely, that the change of membrane voltage was of the same magnitude (4 mV) in all three subpopulations, although in real tissue it would depend on the relative position of neurons with respect to the electrode. The stimulation consisted of square, monophasic pulses of 1 ms duration at the frequency of 10 Hz, delivered during 60 s.

B. Phase clustering index

The phase clustering index (PCI) measures the coherency of phases of different frequency components of the evoked responses and has been used earlier for analysis of auditory responses [11]. The method consists of the following steps:

TABLE I. Model parameters, interpretation, and values.

Parameter	Interpretation	Value
EXC	Amplitude of the average excitatory PSP	Varied from 2.5 to 5 mV in this study
SDI	Amplitude of the average inhibitory PSP (slow dendritic inhibition loop)	Varied from 20 to 50 mV in this study
FSI	Amplitude of the average inhibitory PSP (fast somatic inhibition loop)	20 mV
τ_{EXC}	Time constant of average excitatory postsynaptic potentials	10 ms
τ_{SDI}	Time constant of average slow inhibitory postsynaptic potentials	35 ms
τ_{FSI}	Time constant of average fast inhibitory postsynaptic potentials	5 ms
$C1$, $C2$	Average number of synaptic contacts in the feedback excitatory loop	$C1=C$, $C2=0.8C$ (with $C=135$)
$C3$, $C4$	Average number of synaptic contacts in the slow feedback inhibitory loop	$C3=C4=0.25C$
$C5$, $C6$	Average number of synaptic contacts in the fast feedback inhibitory loop	$C5=C6=0.1C$
$C7$	Average number of synaptic contacts in the connection between slow and fast inhibitory interneurons	$C7=0.8C$
$v0$, $e0$, r	Parameters of the asymmetric sigmoid function S (transforming an average PSP into an average density of action potentials)	$v0=6$ mV $e0=2.5$ s^{-1} $r=0.56$ mV^{-1}
$p(t)$	Excitatory input noise (positive mean Gaussian white noise)	mean=90 pps (pulses per second) std=30 pps

(i) the stimulated signal is divided into single response epochs, (ii) a discrete Fourier transform of each epoch is performed, yielding complex amplitudes of the harmonic frequency components Z_f^s, where f corresponds to frequency and s is a stimulus number, and (iii) the (real-valued) PCI for frequency f is computed as the magnitude of the average of the complex amplitudes, normalized by their average magnitude, over epochs. In the mathematical expressions we denote PCI using the symbol ψ:

$$\psi_f = \left| \frac{\langle Z_f^s \rangle_s}{\sqrt{\langle |Z_f^s|^2 \rangle_s}} \right| . \tag{1}$$

This results in the estimation of the coherency of phases at a given frequency f for response epochs evoked by repetitive stimulation. The PCI index is a normalized quantity approaching 0 for randomly distributed phases and attaining the value of 1 if all phases are equal. The so-called "relative phase clustering index" (rPCI) is defined as the difference between the highest PCI at any of the harmonic frequencies and PCI at the driving (stimulation) frequency. If the difference is negative, the rPCI is set to 0. The detailed description of the PCI measure can be found in [5]. We show in the Appendix that within the framework of the linear response model the PCI can be expressed as

$$\psi_f = \left| \frac{\langle Z_f^s \rangle_s}{\sqrt{\langle |Z_f^s|^2 \rangle_s}} \right| = \left(1 + \frac{S_f^2}{D_f^2} \right)^{(-1/2)} , \tag{2}$$

where S_f is the spectrum of the background activity and D_f is the spectrum of the system's triggered response. Formula (2) relates the PCI to the system's spectral noise-to-signal ratio.

C. Nonlinear association h^2

In addition to the PCI we computed other quantities that characterize signal spectral properties and are considered relevant with respect to seizure prediction. We quantified the degree of association between the "closeness" to seizure in the model and the value of the PCI and of these other quantities. To quantify this association we used a general measure of the interdependence between two signals called nonlinear association or h^2 index [12,13]. This measure quantifies how much of a variation in one signal can be explained based on variation in another signal, without making any assumptions concerning whether their relationship is linear or not.

D. Patient data

To compare model results with experimental data, we used intracranial EEG data from two patients with mesial temporal lobe epilepsy undergoing invasive EEG monitoring as part of their presurgical evaluation. Informed consent was obtained prior to performing the intracranial electrical stimulation studies that were carried out while waiting for the habitual seizures to occur. These data were used in our previous publication [3], and the same patient numbering is preserved here. In the present study, in both patients 3 and 4 we used EEG data from hippocampal electrodes lying in the proximity of the seizure onset site as determined from visual inspection of preictal and ictal EEG recordings.

III. RESULTS

A. Active and passive paradigm in the model

We computed S_f and D_f separately in order to assess their relative contribution to the PCI and also to quantify their potential ability to detect changes of excitability of the network. In the model the background activity during stimulation and the spontaneous activity in the absence of the stimulus are practically the same. As a single value estimate of the background activity, we can take therefore the standard deviation of the spontaneous output signal. It represents the contribution of all spectral components of the spontaneous spectrum S_f that can be measured directly from nonstimulated signals. We term this quantity S_0. Additionally, as a

single-value estimate of the system's triggered response, we selected D_1, the spectral component of the triggered response corresponding to the driving frequency.

B. Seizure threshold

The seizure threshold in the model was quantified as the minimal amount of increase of the mean rate of the afferent action potentials necessary for the network to switch behavior from low-amplitude normal ongoing activity to high-amplitude limit-cycle oscillations; the latter are assumed to correspond to seizure activity in real situations. It is often considered that seizure generation depends, in global terms, on the balance between excitatory and inhibitory processes of the underlying network [14,15]. In the model two types of inhibition coexist: a slow and a fast inhibition mediated by the two distinct populations of interneurons targeting $GABA_A$ receptors located either in the dendritic or in the somatic region of pyramidal cells, respectively [16]. In the model we targeted primarily the slow dendritic inhibition as the relevant factor regarding the propensity for seizure occurrence, since it was shown that this kind of inhibition is affected in epileptic hippocampus [17]. Therefore we investigated how the seizure threshold in the model depends on the two parameters EXC and SDI, which correspond to the amplitudes of the average excitatory and slow dendritic inhibitory postsynaptic potentials, respectively. The EXC parameter was varied from 2.5 to 5 mV in steps of 0.125 mV; the SDI parameter was varied in the range of 20 to 50 mV in steps of 1 mV. The seizure threshold was measured for each pair of EXC and SDI values. Results of the simulations are shown in Fig. 2(a). The seizure threshold is represented along the vertical axis and by the color of the three-dimensional surface. It can be seen that the seizure threshold depends on both parameters EXC and SDI. As one may expect, low overall excitation and high inhibition result in a high threshold (light color), while increasing values of EXC and decreasing values of SDI result in a lowering of the threshold (dark red color). During the seizure threshold analysis, the noise component was removed from the input to improve clarity of the presentation. With the noise component present, the parameter settings for the lowest threshold resulted in isolated interictal spikes occasionally emerging out of a normal background. These parameter settings were excluded from further analysis.

C. Behavior of possible seizure "predictors"

The relationship between the values of the seizure predictors S_0, D_1, and rPCI and the seizure threshold can be examined from the plots presented in Figs. 2(b)–2(d). In these plots the color code corresponds to the value of seizure threshold, as in Fig. 2(a). It can be seen that both S_0 and D_1 are poor predictors since low seizure threshold values (dark red area) correspond to a wide range of values of these two possible seizure predictors. Furthermore, it appears that S_0 and EXC are approximately linearly related, while S_0 is little influenced by SDI [Fig. 2(b)]; similarly, D_1 is little influenced by EXC, and a linear relation is also apparent for the relationship between D_1 and SDI. The behavior of the rPCI

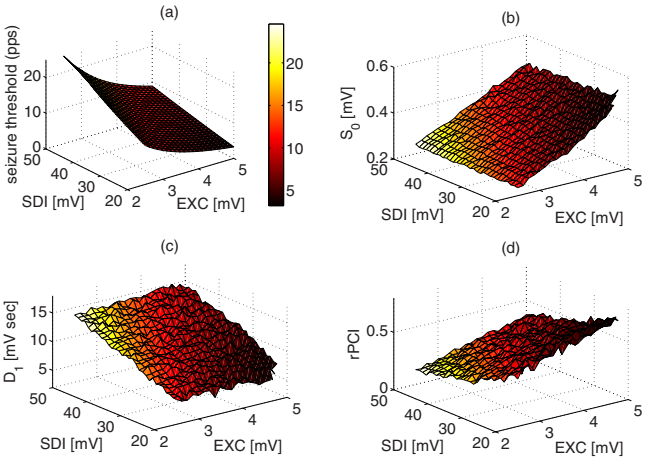

FIG. 2. (Color online) Dependence of the model properties (z axis and color) on SDI (x axis) and EXC (y axis) parameters. In all four plots the color scale corresponds to the value of the seizure threshold. (a) Dependence of the seizure threshold [in pulses per second (pps)] and a color bar showing the color scale used. (b) Dependence of the standard deviation of spontaneous activity S_0. One can see that this measure is sensitive only to a change of the EXC, but not to a change of the SDI parameter. (c) Dependence of the system's triggered response D_1. One can see that this measure is sensitive only to a change of the SDI, but not to a change of the EXC parameter. (d) Dependence of the rPCI showing that this measure is sensitive to a change of both the EXC and SDI parameters.

is different. Low threshold values correspond to relatively large values of the rPCI. These results show that the rPCI is a more robust seizure predictor than the other features investigated here.

In addition, we quantified the relationship between the value of seizure predictors and seizure threshold using the h^2 association index. Figures 3(a)–3(c) show the scatter plots between the model's seizure threshold and different seizure predictors along with corresponding h^2 values. The nonlinear association measures computed for the D_1 and S_0 predictors (h^2=0.3 and 0.64, respectively) were lower than that for the rPCI predictor (h^2=0.94). Figure 3(d) shows the scatter plot of rPCI values versus time to seizure and the corresponding h^2 value for the case of the EEG signal of an epileptic temporal lobe patient (patient 3; see [3]). One can notice that low PCI values (about $<$0.3) correspond to long "times to seizures," while large values (about $>$0.4) correspond to short "times to seizures." A comparison between Figs. 3(c) and 3(d) allows us to draw a rough parallel between the gradual increase of the rPCI value and the decrease of the seizure threshold, as estimated using the model, on the one hand [Fig. 3(c)], and the time to seizure in the real patient data, on the other hand [Fig. 3(d)].

D. Comparison with experimental data

In order to examine how the parameters S_0, D_1, and rPCI behave when applied to real EEG data, we constructed the time courses of these parameters in two patients with TLE. Results are shown in Fig. 4. In patient 3 the S_0 parameter changed little throughout the observation period, while the

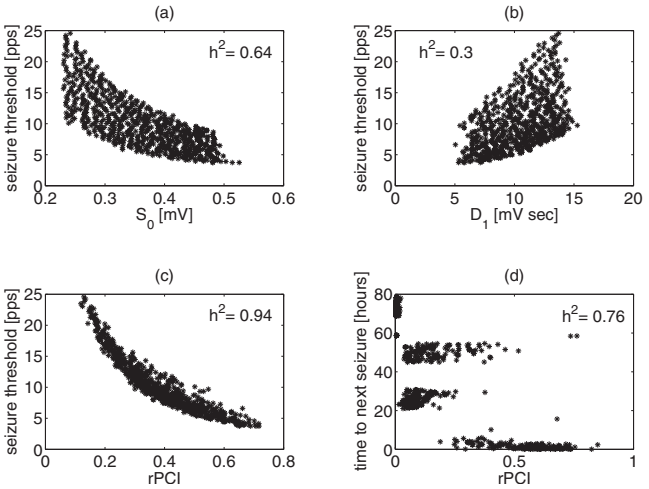

FIG. 3. (a), (b), (c) Scatter plots of the seizure threshold [pulses per second (pps)] and measurable quantities (S_0, D_1, and rPCI, respectively) obtained for all pairs of the EXC and SDI parameters in the model. In each graph, the value of nonlinear association measure h^2 is used to quantify the correlation between the respective variables. The h^2 values show that the rPCI measure is best correlated with the seizure threshold, while its scatter-plot hyperbolic shape resembles that of the real data. (d) Scatter plot of the time to next seizure and rPCI value in a TLE patient (patient 3 described in [3]).

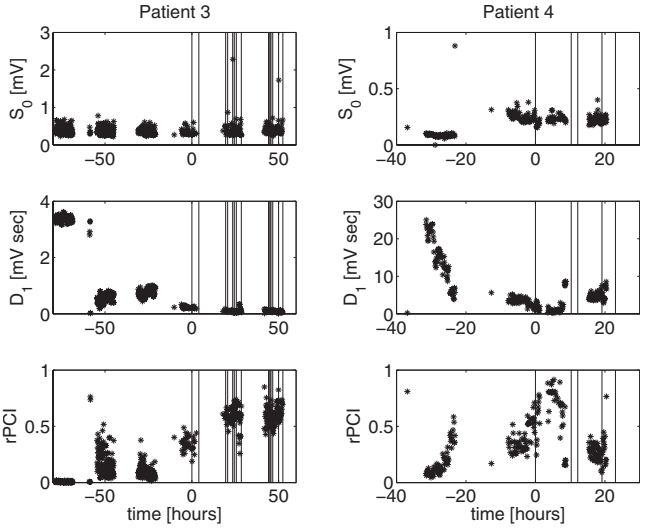

FIG. 4. Examples of time evolution of the S_0, D_1, and rPCI in two TLE patients. Points denote measurements, while the vertical bars denote seizures. The inhomogeneous structure of the plots is due to the fact that data were collected in these cases mainly during the night. In patient 3, the S_0 does not change towards seizures, while there is a marked decrease of the D_1 parameter and increase of the rPCI parameter. In patient 4, there is an increase of the S_0 parameter toward seizures. The D_1 parameter initially decreases, but starts to increase after the first seizure. The rPCI parameter initially increases up to few hours after first seizure and starts to decrease afterwards.

D_1 parameter decreased markedly at the beginning of the observation period, long before the first seizure (i.e., the first seizure recorded following antiepileptic drug withdrawal during monitoring) and thereafter remained low, reaching a minimum just before the seizure and remained at this low value during subsequent seizures. The rPCI started to clearly increase some time before the first seizure and increased further during subsequent seizures. In patient 4 the S_0 parameter increased before the first seizure and remained at about the same level for the remaining observation period. The D_1 parameter decreased very much long before the first seizure and remained low, but without many changes, when seizures occurred. The rPCI increased as D_1 decreased far from the first seizure, but later it increased gradually a few hours before the seizure, remained high thereafter, and then decreased before the last observed seizures.

E. rPCI for high and low excitability

The model gives us the possibility of obtaining insight into the significance of the rPCI in terms of the parameters which play an essential role in the control of the excitability of the neuronal network and thus in the transition between normal and seizure activity. For this purpose we considered three different ways by which the normal state, characterized by (i) normal inhibition and normal excitation, may change into a state of enhanced excitability characterized by (ii) high Excitation, (iii) low Inhibition, or (iv) a combination of both. The latter condition corresponds to the most excitable state—i.e., the lowest seizure threshold. For these four parameter settings we investigated a number of features that can be extracted from the model spontaneous output and from the triggered response signal. These features include the power spectra, the PCI values, and the distribution of phases of triggered responses from which the rPCI value is derived. The results are shown in Fig. 5. The four panels in part (a) of the figure show the model output—i.e., the mean membrane potential of the main cells' population for four different conditions. One can notice that as one goes from the normal condition (i), through the conditions of high Excitation (ii), low Inhibition (iii), into highest excitability (iv), the DC of the mean membrane potential increases, which results in a progressive decrease of the seizure threshold. However, this change in excitability is not accurately reflected in the signal variance. The transition from a normal to a high Excitation condition leads to an increased amplitude of the spontaneous activity, while the transition into the low Inhibition condition has no influence on the variance of the output signal. This is also put into evidence by the power spectra of the spontaneous activity shown in part (b) of Fig. 5. The spectral magnitudes under (i) normal conditions (blue crosses) overlap perfectly with signal's power spectrum under conditions of (iii) low Inhibition (yellow circles). Similarly, both spectral magnitudes under both high Excitation conditions [(ii) and (iv)] overlap (green squares and red dots) regardless the difference in the level of inhibition. In contrast, the average spectra of the triggered responses shown in the right panel, part (b) of Fig. 5, are sensitive to the levels of both excitation and inhibition; this is especially clear when the inhibition is low. Under this condition [(iii) and (iv)], the difference in spectra (yellow circles and red dots) is most pronounced. However, for a normal level of inhibition [(i)

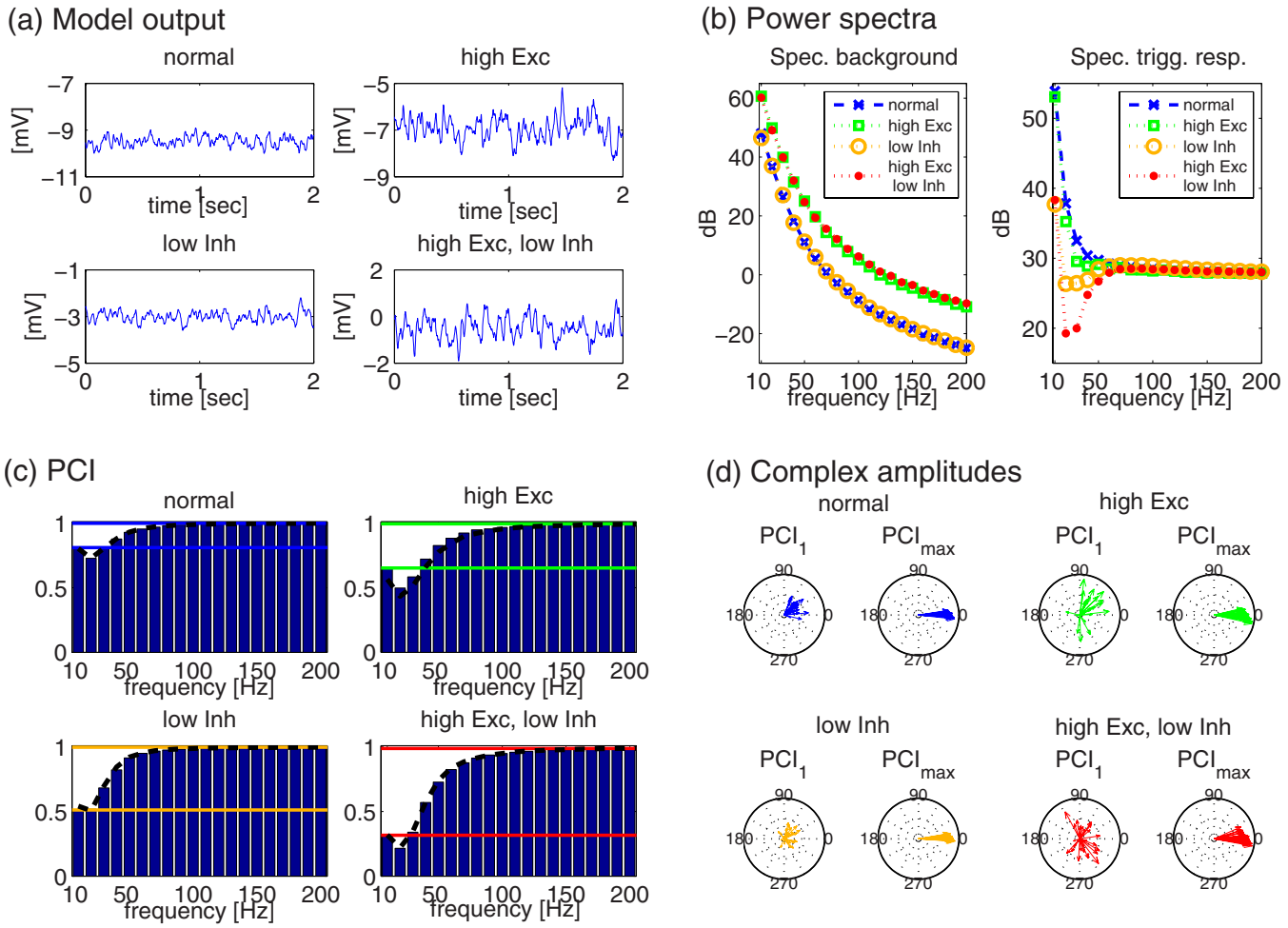

FIG. 5. (Color online) Model-based interpretation of the relationship between the PCI and the level of excitability. In each part (a), (b), (c), and (d) of this figure, different variables are plotted for four different conditions. Simulations of normal conditions ("normal") were performed with EXC=2.5 mV and SDI=50 mV; increased excitability due to increased excitation ("high Exc") was simulated using EXC=4.75 mV and SDI=50 mV; increased excitability due to decreased inhibition ("low Inh") was simulated using EXC=2.5 mV and SDI=22 mV; and highest excitability ("high Exc, low Inh") was simulated using EXC=4.75 mV and SDI=22 mV. In all simulations the external stimulation input was a 10-Hz sequence of 60 monophasic pulses of 1 ms duration. (a) Spontaneous model output for different excitability conditions. Different parameter settings result in different DC offsets of the signals; "normal," −9.45 mV; "high Exc," −7 mV; "low Inh," −3 mV; "high Exc, low Inh," −0.52 mV. Increased excitation (upper right panel) leads to increased signal variance, while lowered inhibition (lower left side panel) has no significant influence on the signal variance. (b) Average power spectra of spontaneous and triggered activity. In both cases the spectra were computed by dividing the signal (in the spontaneous case artificial "triggers" were introduced) into segments corresponding to single response epochs (100 ms) and removing the DC offset of each epoch. For spontaneous spectra the magnitudes obtained from discrete Fourier transform of the epochs were averaged across all epochs and plotted along a logarithmic (dB) scale. For triggered spectra, the average of complex amplitudes of Fourier-transformed triggered responses over all epochs was computed and its magnitude was plotted. In each panel, spectra corresponding to different excitability conditions are plotted with different colors and markers: "normal," blue crosses; "high Exc," green squares; "low Inh," yellow circles; "high Exc, low Inh," red dots. Spontaneous spectra of "normal" and "low Inh" as well as those of "high Exc" and "high Exc, low Inh" overlap with each other, implying that level of inhibition has no influence on spectral power of background activity at any frequency. The spectra of triggered responses are distinct for changes of excitation and inhibition. (c) Spectrum of phase clustering index. Phase coherencies at a given frequency were computed directly from the spread of phases of complex amplitudes obtained by Fourier transform of triggered responses (blue bars) and using Eq. (2) (black dashed line). Values of the PCI at the driving frequency (PCI_1) and at the frequency at which the PCI has maximal value (PCI_{max}) are marked with horizontal lines of colors corresponding to the color code used in spectral plots in part (b). The distance between the lines corresponds to the value of rPCI. The rPCI values increase for increasing DC levels of the output signals shown in part (a). (d) Complex amplitudes. Polar plots of amplitudes of Fourier-transformed triggered responses at the driving frequency and at which the PCI is maximal. Color of the arrows corresponds to the color code used in parts (b) and (c). Only amplitudes from the first 25 triggered responses are shown for clarity. While the spread of phases—i.e., the variability of the arrow directions—is small for PCI_{max} for all four conditions, the degree of phase scattering at the driving frequency, as quantified by PCI_1, differs between the conditions studied.

and (ii)] the distinction between triggered responses spectra (blue crosses and green squares) is less prominent. The difference between all four conditions can be most clearly seen in the phase clustering index plots in part (c) of the figure. The PCI computed directly from the distribution of phases of triggered responses at the driving and higher harmonic frequencies is plotted as vertical bars. On each plot are superimposed PCI curves computed by way of formula (2) using the spontaneous spectrum, instead of the spectrum of background fluctuations, S_f. As can be seen, all four PCI spectra are close to the value 1 for higher frequencies (>100 Hz). This is due to the fact that background activity has very little power in this frequency range [note that spectral magnitudes in part (b) are plotted in logarithmic scale] and does not affect phase coherency. On the contrary, at the lower side of the frequency spectrum all four PCI spectra differ markedly. This is because the amplitudes of excitatory and inhibitory postsynaptic potentials, which have time constants in the order of tens of milliseconds, influence spectral properties of the system mainly at the low-frequency range (<100 Hz). In general, we should note that both a high spectral magnitude of background activity and a low spectral magnitude of triggered responses cause a lowering of the phase coherency [see Eq. (2)]. Indeed, the lowest PCI values are attained for the condition of high Excitation and low Inhibition, for which the background spectrum is relatively high and the triggered spectrum is the lowest among all the four spectra. On the contrary, the highest PCI values are obtained for the normal excitability conditions. The single-value quantifier of the PCI spectrum, the relative PCI or rPCI, is defined as the difference between the highest PCI at any of the harmonic frequencies and PCI at the stimulation frequency. In PCI histograms [Fig. 5(c)], the maximal value of the PCI, $\mathrm{PCI}_{\max}$, and the PCI at the stimulation frequency, PCI_1, are marked by two horizontal lines in colors corresponding to those used in the plot of the corresponding power spectra. The distance between the two lines corresponds to rPCI. One can see that the value of rPCI increases from the normal condition to the other conditions along with the decrease of seizure threshold. Part (d) of the figure shows polar plots of the complex amplitudes of the triggered responses for the two frequency components for which the rPCI was computed. The length of each arrow corresponds to the magnitude of the Fourier-transformed triggered response at a given frequency, while the angle corresponds to its phase relative to the stimulus. One can notice that whereas the distribution of phases corresponding to $\mathrm{PCI}_{\max}$ is rather tight for all four conditions, the phases at the stimulation frequency are aligned for the normal conditions, but they are randomly scattered for the condition of highest excitability. Thus, in the model, an increase of phase variability at the driving frequency is mainly responsible for the increase of the rPCI value that is associated with lowering the seizure threshold.

IV. DISCUSSION

Complex partial seizures are the most common seizure type [18], while 60% of them originate in the hippocampus and surrounding mesial temporal structures [19]. We used a computer model of the hippocampal network to test in a controlled way the behavior of different indices that can be used to follow dynamical changes of EEG signals as the transition to a seizure approaches. It is generally believed that the processes that lead to epilepsy (i.e., epileptogenesis) are related to a shift of the balance between excitation and inhibition [14]. It has been shown *in vitro* [15] that in the CA1 area of the epileptic hippocampus the glutamatergic drive was increased in soma of pyramidal cells, while the GABAergic drive was decreased in dendrites. Furthermore, using animal models of TLE, it has been shown that excitatory synaptic activity was increased in pyramidal cells in epileptic animals [20], while GABAergic inhibition was reduced in dendrites, but not in soma of pyramidal cells [17]. It should be noted that a change in synaptic activity may result from alterations in synaptic current properties, such as decay and rise-time constants or current amplitude, or from synaptic reorganization—e.g., formation of new recurrent excitatory circuits and/or loss of inhibitory cells. We mapped the microscopic glutamatergic and GABAergic activity changes in the CA1 region into only two macroscopic parameters: the amplitude of the average excitatory postsynaptic potential, EXC, and the amplitude of the average slow Inhibitory postsynaptic potential, SDI. It should be noted, however, that in our model synaptic potential amplitudes are multiplied by coupling constants C; thus, a change of EXC or SDI is equivalent to a change in the average number of synaptic contacts. For that reason, although we cannot investigate local interactions between individual cells, we are able to capture global changes in synaptic network connectivity. Although our model assumptions may be violated in specific experimental conditions, they should hold in general when dealing with the overall behavior of interacting populations of neurons. Using two parameter analyses, we showed that both excitatory and slow Inhibitory synaptic transmissions were critical with respect to setting the seizure threshold in the model [Fig. 2(a)]. We may assume that in the real system during ictogenesis these two parameters change over time, progressively reducing the system's stability and ultimately leading to an ictal transition. Hence, we compared the ability of different EEG indices to detect changes of excitation and inhibition in the modeled hippocampal network. We found that the change of excitation could be accurately detected by the standard deviation of the spontaneous activity, while the change of inhibition was not reflected in this variable [Fig. 2(b)]. On the other hand, the spectral variable corresponding to the evoked response changed markedly with the level of inhibition, but it was not sensitive to the change of excitation [Fig. 2(c)]. The rPCI being a combination of the spontaneous and evoked activities was sensitive to changes of both EXC and SDI parameters [Fig. 2(d)]. To quantify the ability of the three measures investigated here, rPCI, S_0, and D_1, regarding their potential use for seizure anticipation, we computed the nonlinear correlation index h^2 between the seizure threshold and the values of the three measures for all possible pairs of EXC and SDI parameters. The correlation index for the rPCI measure was higher than that for both the S_0 and D_1 measures (Fig. 3). These results imply that purely passive observations of the system do not reliably detect changes underlying a transition to a seizure. The most reliable way to

detect these changes is to apply an active stimulation paradigm. On the other hand, by monitoring separately changes in spontaneous and evoked activity, e.g., by means of mixed active-passive paradigms, it might be possible to reconstruct processes at the neuronal level that are responsible for ictal transitions in a given patient. The model predicts that changes in spontaneous activity, measured by the S_0 parameter, would be primarily related to alterations in the excitatory synaptic component, while changes in the evoked activity, measured by the D_1 parameter, would reflect mainly the breakdown of inhibitory mechanisms. Two examples of the time evolution of the S_0, D_1, and rPCI measures in epileptic TLE patients are shown in Fig. 4. The relatively fixed value of the S_0 parameter throughout the observation period in patient 3 suggests that in this patient the level of excitation remained constant. On the other hand, a pronounced decrease of the D_1 parameter suggests that progressive lowering of inhibition, possibly due to tapering of the antiepileptic drug during monitoring, was a primary factor leading to seizures (vertical lines). In patient 4 the marked decrease of the D_1 parameter occurred together with the increase of the S_0 parameter. It suggests that changes of both excitation and inhibition played a role in shifting the balance of the system towards the first ictal transition. Interestingly, in this patient, the D_1 parameter decreased and the rPCI increased only up to a few hours after the first seizure. Shortly afterwards, the reverse changes were observed. This shows that the first seizure may alter the conditions for the generation of the subsequent seizures, which may pose a limitation of the ability of rPCI, and other indices as well, to predict seizures that occur in clusters in some patients. The present model study not only demonstrates that it is useful to perform stimulation in order to obtain the necessary information about the system dynamics and its evolution towards the state of high probability of ictal transition (*proictal* state), but it also allows one to explain *why* we need to stimulate. In general, an extracellular time-varying signal reflects the transfer function of the local neural network only if the network is subjected to a flat spectrum—e.g., white noise, input. As described, e.g., in [21], a number of stochastic processes at the microscopic level can be considered as noise sources contributing to random fluctuations of noise input signals at the macroscopic level. One should realize that the white noise is a theoretical idealization and does not exist in real neural networks because these networks have filtering properties. Even if one assumes a white noise input, as in the present model, the high-frequency content of the input signal is attenuated already at the first excitatory synaptic connection (see Fig. 1) and therefore it cannot fully reveal the state of the other parts of the network, e.g., resulting from the inhibitory feedback loop. External stimulation perturbing all parts of the network using a flat spectrum input is therefore likely to reveal more information about local network properties. From the above discussion it follows that the effective stimulation should have flat spectrum characteristics, but it is not essential that it be delivered periodically. Furthermore, as far as only spectral (i.e., linear) properties are concerned, we may predict that white noise input applied externally should perform equally good as pulse stimulation as we verified using the model (not shown). Therefore the stimulation sequence does not need to be "fine-tuned" to a specific critical frequency or pattern, which increases the universality of the method. The location of the stimulation input within the system, on the contrary, can be of significance for the state reconstruction performance of the rPCI quantity. As we can show theoretically, stimulation applied along the same pathway as the external "noise" is fed to the system would result in constant rPCI values, independent of the system's state.

Finally, we propose a model-based interpretation of the experimental results that motivated the present study—i.e., that an increase of the rPCI anticipates transitions to epileptic seizures in TLE patients (Fig. 5). Additionally, we verified numerically the relationship between PCI and the ratio between the triggered response spectrum and the spectrum of background fluctuations of the stimulated system, expressed by formula (2). The spectrum of background fluctuations, S_f, was approximated here by the spontaneous spectrum; nonetheless, the relationship was preserved [Fig. 5(c)], suggesting that deviations from the linear response model are negligible in these cases, and therefore purely linear effects may account for the rPCI seizure predictive power in the model and possibly also in real systems.

ACKNOWLEDGMENTS

P.S. was partly supported by Polish funds for science, Grant No. N407 041 32/1646.

APPENDIX

In this appendix the expression for PCI in the framework of the linear response model is derived.

The response of a linear system to a stimulus can be represented in the following general form:

$$Z_f^s = T_f^s x_f^s + Q_f^s, \tag{A1}$$

where x_f^s are the Fourier amplitudes of the stimulus, T_f^s represent input-output transfer functions, and Q_f^s represent internal functions reflecting the background activity. We assume that both the stimulation and the system's transfer functions are stationary—i.e., $x_f^s = x_f$ and $T_f^s = T_f$ for all stimuli. We define the triggered response spectral power function as a stimulus average of (A1):

$$D_f^2 \equiv |\langle Z_f^s \rangle_s|^2 = |T_f|^2 |x_f|^2. \tag{A2}$$

In deriving (A2) we assumed that the internal fluctuations are uncorrelated to the stimulus and $\langle Q_f^s \rangle_s \approx 0$. Next, we average the square magnitude of (A1), assuming again that the background activity is uncorrelated to the stimulus and the system's response:

$$A_f^2 \equiv \langle |Z_f^s|^2 \rangle_s = D_f^2 + S_f^2. \tag{A3}$$

Here we have introduced the power spectrum of background fluctuations as

$$S_f^2 \equiv \langle |Q_f^s|^2 \rangle_s. \tag{A4}$$

Finally, substituting (A2) and (A3) into expression for PCI (1), we get

$$\psi_f = \left| \frac{\langle Z_f^s \rangle_s}{\sqrt{\langle |Z_f^s|^2 \rangle_s}} \right| = \left(1 + \frac{S_f^2}{D_f^2} \right)^{(-1/2)}. \tag{A5}$$

The above formula gives the relationship between the PCI and the noise-to-signal ratio of the stimulated system.

[1] K. Lehnertz, F. Mormann, H. Osterhage, A. Muller, J. Prusseit, A. Chernihovskyi, M. Staniek, D. Krug, S. Bialonski, and C. E. Elger, J. Clin. Neurophysiol. **24**, 147 (2007).

[2] F. Mormann, R. G. Andrzejak, C. E. Elger, and K. Lehnertz, Brain **130**, 314 (2007).

[3] S. Kalitzin, D. Velis, P. Suffczynski, J. Parra, and F. L. Lopes da Silva, Clin. Neurophysiol. **116**, 718 (2005).

[4] S. Wong, A. B. Gardner, A. M. Krieger, and B. Litt, J. Neurophysiol. **97**, 2525 (2007).

[5] S. Kalitzin, J. Parra, D. Velis, and F. H. Lopes da Silva, IEEE Trans. Biomed. Eng. **49**, 1279 (2002).

[6] J. Parra, S. Kalitzin, J. Iriarte, W. Blanes, D. Velis, and F. H. Lopes da Silva, Brain **126**, 1164 (2003).

[7] F. Wendling, F. Bartolomei, J. J. Bellanger, and P. Chauvel, Eur. J. Neurosci. **15**, 1499 (2002).

[8] F. Wendling, A. Hernandez, J. J. Bellanger, P. Chauvel, and F. Bartolomei, J. Clin. Neurophysiol. **22**, 343 (2005).

[9] A. van Rotterdam, F. H. Lopes da Silva, J. van den Ende, M. A. Viergever, and A. J. Hermans, Bull. Math. Biol. **44**, 283 (1982).

[10] http://senselab.med.yale.edu/ModelDB/ShowModel.asp?model=97983

[11] R. A. Dobie and M. J. Wilson, Electroencephalogr. Clin. Neurophysiol. **92**, 405 (1994).

[12] F. H. Lopes da Silva, J. P. Pijn, and P. Boeijinga, Brain Topogr **2**, 9 (1989).

[13] S. Kalitzin, J. Parra, D. Velis, and F. H. Lopes da Silva, IEEE Trans. Biomed. Eng. **54**, 454 (2007).

[14] F. H. Lopes da Silva, J. P. Pijn, and W. J. Wadman, Prog. Brain Res. **102**, 359 (1994).

[15] L. El-Hassar, M. Milh, F. Wendling, N. Ferrand, M. Esclapez, and C. Bernard, J. Physiol. (London) **578**, 193 (2007).

[16] M. I. Banks, J. A. White, and R. A. Pearce, Neuron **25**, 449 (2000).

[17] R. Cossart, C. Dinocourt, J. C. Hirsch, A. Merchan-Perez, J. De Felipe, Y. Ben-Ari, M. Esclapez, and C. Bernard, Nat. Neurosci. **4**, 52 (2001).

[18] H. Gastaut, J. L. Gastaut, G. E. Gonçalves de Silva, and G. R. Fernandez Sanchez, Epilepsia **16**, 457 (1975).

[19] P. D. Williamson, http://www.ilae-epilepsy.org/Visitors/Centre/ctf/mesial_temp_lobe.html.

[20] L. R. Shao and F. E. Dudek, J. Neurophysiol. **92**, 1366 (2004).

[21] F. H. Lopes da Silva, J. P. Pijn, D. Velis, and P. C. Nijssen, Int. J. Psychophysiol **26**, 237 (1997).